Journal Pre-proof

Characterization of the starch surface binding site on Bacillus paralicheniformis α-amylase

Nataša Božić, Henriëtte J. Rozeboom, Nikola Lončar, Marinela Šokarda Slavić, Dick B. Janssen, Zoran Vujčić

PII: S0141-8130(20)34647-X

DOI: https://doi.org/10.1016/j.ijbiomac.2020.10.025

Reference: BIOMAC 16915

To appear in: *International Journal of Biological Macromolecules*

Received date: 5 August 2020

Revised date: 3 October 2020

Accepted date: 3 October 2020

Please cite this article as: N. Božić, H.J. Rozeboom, N. Lončar, et al., Characterization of the starch surface binding site on Bacillus paralicheniformis α-amylase, *International Journal of Biological Macromolecules* (2018), https://doi.org/10.1016/j.ijbiomac.2020.10.025

This is a PDF file of an article that has undergone enhancements after acceptance, such as the addition of a cover page and metadata, and formatting for readability, but it is not yet the definitive version of record. This version will undergo additional copyediting, typesetting and review before it is published in its final form, but we are providing this version to give early visibility of the article. Please note that, during the production process, errors may be discovered which could affect the content, and all legal disclaimers that apply to the journal pertain.

© 2018 Published by Elsevier.

Characterization of the starch surface binding site on *Bacillus paralicheniformis* α-amylase

Nataša Božić[1a*], Henriëtte J. Rozeboom[2a], Nikola Lončar[3], Marinela Šokarda Slavić[1], Dick B. Janssen[2] and Zoran Vujčić[4]

[1]Department of Chemistry, Institute of Chemistry, Technology and Metallurgy, National Institute of the Republic of Serbia, University of Belgrade, Studentski trg 12-16, 11000 Belgrade, Serbia
[2]Groningen Biomolecular Sciences and Biotechnology Institute, University of Groningen, Nijenborgh 4, 9747AG Groningen, the Netherlands
[3]GECCO Biotech, Nijenborgh 4, Groningen, 9747AG, the Netherlands
[4]Department of Biochemistry, Faculty of Chemistry, University of Belgrade, Studentski trg 12-16, 11000 Belgrade, Serbia
[a]These two authors contributed equally to this work
*Corresponding author at: Department of Chemistry, Institute of Chemistry, Technology and Metallurgy, University of Belgrade, Studentski trg 12-16, 11000 Belgrade, Serbia. Tel.: +381 113282393; fax: +381 112636061. E-mail address: nbozic@chem.bg.ac.rs.

Highlights

Structure determination of *Bacillus paralicheniformis* α-amylase ATCC 9945a

Binding of four different oligosaccharides and oligosaccharide precursors

Confirmation of the unusual starch binding site on the α-amylase

Verification of the starch binding site by mutational analysis

Abstract

α-Amylase from *Bacillus paralicheniformis* (*Bli*Amy), belonging to GH13_5 subfamily of glycoside hydrolases, was proven to be a highly efficient raw starch digesting enzyme. The ability of some α-amylases to hydrolyze raw starch is related to the existence of surface binding sites (SBSs) for polysaccharides that can be distant from the active site. Crystallographic studies performed on *Bli*Amy in the apo form and of enzyme bound with different oligosaccharides and oligosaccharide precursors revealed binding of these ligands to one SBS with two amino acids F257 and Y358 mainly involved in complex formation. The role of this SBS in starch binding and degradation was probed by designing enzyme variants mutated in this region (F257A and Y358A). Kinetic studies with different substrates show that starch binding through the SBS is disrupted in the mutants and that F257 and Y358 contributed cumulatively to binding and hydrolysis. Mutation of both sites (F257A/Y358A) resulted in a 5-fold lower efficacy with raw starch as substrate and at least 5.5-fold weaker binding compared to the wild type *Bli*Amy, suggesting that the ability of *Bli*Amy to hydrolyze raw starch with high efficiency is related to the level of its adsorption onto starch granules.

Keywords: α-amylase, crystal structure, starch, surface binding site, mutant

Journal Pre-proof

1. INTRODUCTION

Industrially relevant polysaccharides are complex structures that can be enzymatically degraded by glycoside hydrolases (GHs). Starch is one of the most important polysaccharides for humans both in food and non-food applications, such as for bioethanol production, drug delivery, and in the paper and textile industries [1, 2]. As a component of dietary intake, raw starch behaves as resistant starch. It escapes digestion and absorption in the small intestine and is fermented in the large intestine by microorganisms, with production of short-chain fatty acids. There is now abundant evidence showing that short-chain fatty acids play an important role in sustaining health and that their formation and uptake may lower the risk of disease [3].

The possibility of raw starch hydrolysis would be a major breakthrough in the starch processing industry, since the overall cost of producing starch-based products might be reduced through energy savings and by more effective use of starch-containing resources [4-6]. Amylases able to degrade granular or native starch below the gelatinization temperature of starch are known as raw starch degrading amylases (RSDA) and can be found in species from all kingdoms of life. Understanding the ability of such amylases to degrade raw starch will support their applicability in the starch-processing industry, with potential health benefits of food products [7].

Enzymes active towards polysaccharides exhibit different strategies for cleavage of raw starch. The most common solution is the presence of starch-binding regions that are distinct from the active site yet facilitate the action of the enzyme by a proximity effect that can at the structural level include directing the substrate chain towards the catalytic site. This non-catalytic carbohydrate binding is achieved either through additional carbohydrate-binding modules (CBMs) often located at separate domains that are connected to the catalytic domain by a polypeptide linker or *via* one or more surface binding sites of the catalytic domain itself (SBSs, sometimes called secondary binding site). The structures and functions of CBMs have been extensively studied [8-11], and recently comprehensive review of starch binding domains (sometimes referred to as SBDs) was published [12], but there is a lack of information on SBSs since they occur less frequent and cannot be easily identified from sequence similarity studies. SBSs are usually found only by structural studies. So far, approximately 60 enzymes from 20 CAZy (www.cazy.org) families were found to possess one or more SBSs [13], and almost half of these enzymes belong to GH13 α-amylase family. Examination of X-ray structures obtained from α-amylase crystals soaked or co-crystallized with substrates or substrate analogs revealed the presence of SBSs separate from the active site. However, studies to elucidate their functional significance have been done in only a few cases [14-17].

Literature on the role of SBSs has been recently reviewed [18, 19], including papers with emphasis on GH13 α-amylase family [20, 21]. Several SBSs have been described in enzymes participating in starch degradation. For the hydrolysis of raw starch physical adsorption of amylolytic enzymes is often referred to as *conditio sine qua non.* Most likely the role of SBS is related to the processivity of the enzymes: localization of the enzyme on the polymeric substrate

enabling the active site to perform multiple catalytic cycles without dissociation of the enzyme from the ES complex [17]. Other important roles of SBSs include disruption of the complex carbohydrate structure, guidance of the polymer strand into the active site, and allosteric regulation [19].

Recently, a thermostable and highly efficient RSDA from *Bacillus licheniformis* ATCC 9945a (*Bli*Amy) was described [22]. The enzyme was overproduced in high yield in *E. coli* and could efficiently hydrolyze highly concentrated raw corn starch, showing its potential value for starch-processing industries [23]. Whereas some bacterial α-amylases are capable of hydrolysis of raw starches at high concentration (30 % w/v) [24-26], *Bli*Amy accomplished complete hydrolysis of 91 % upon prolonged incubation [23]. *Bli*Amy was more efficient than α-amylase from *Anoxybacillus flavothermus* which lead to 77 % hydrolysis of a 31 % raw corn starch suspension after 96 h at 61°C [24] or α-amylase from *Geobacillus thermoleovorans* that hydrolysed 40 % of raw corn starch (30 % slurry) at 60°C [25].

The enzyme belongs to the GH13_5 family of α-amylases (EC 3.2.1.1), which share a typical tertiary structure consisting of three distinct domains called A, B and C. The catalytic activity is located in the A domain which has a $(\beta/\alpha)_8$ (TIM-barrel) structure [27, 28]. There is no separate carbohydrate- or starch-binding domain and structural features that contribute to the high activity with raw starch are unclear. Furthermore, no crystal structures of ligand complexes of *Bli*Amy are available.Consequently, in this work we seek to elucidate whether the highly efficient raw starch digestion activity of *Bli*Amy is influenced by other interactions with starch, e.g. by the presence of starch-binding sequences in the catalytic domain or elsewhere in the protein. Using X-ray crystallography studies with different ligands, we identified an SBS on the surface of the catalytic A domain of *Bli*Amy. The role of this SBS was investigated by kinetic studies with different substrates and with *Bli*Amy variants carrying mutations in the SBS region. We show that the ability of *Bli*Amy to hydrolyze raw starch with high efficiency is related to adsorption of the enzyme onto the starch granule mediated by this SBS.

2. MATERIAL AND METHODS

2.1 Protein preparation for crystallography: The untagged wild-type *Bli*Amy protein (GenBank accession number JN042159) was overexpressed and purified as previously described [23, 29]. Purity (>95%) was checked by sodium dodecyl sulfate−polyacrylamide gel electrophoresis (SDS-PAGE). The protein was concentrated to 3 mg/mL in a buffer solution containing 25 mM HEPES (pH 7.5) and 10% (v/v) glycerol.

2.2 Protein preparation for biochemical characterization: Wild-type *Bli*Amy and mutants were expressed with an N-terminal 6xHis-tag and purified using a standard IMAC procedure on Ni-Sepharose. Briefly, enzymes were overexpressed and purified according to the following procedure: an overnight culture in LB medium with ampicillin of *E. coli* NEB10β cells carrying the desired plasmid was diluted 100-fold into 400 mL TB medium with 50 µg/mL ampicillin (TB_{amp}) in 2 L baffled flasks (Sigma Aldrich). Cells were induced at OD_{600} = 2 by adding

0.02% (w/v) L-arabinose (final concentration) and incubation was continued at 24 °C for 40 h (135 rpm). Cells were harvested by centrifugation at 6000 rpm at 4 °C for 20 min. Cell pellet was then resuspended in 50 mM potassium phosphate (KPi) buffer, pH 8.0. To prevent unwanted proteolysis 0.1 mM phenylmethylsulfonyl fluoride was added to the extraction buffer. Cells were disrupted by sonication and centrifuged at 4 °C 12,000 rpm for 60 min. The cell-free extract was applied on a 4 mL Ni-Sepharose FF gravity column pre-equilibrated in 50 mM KPi buffer pH 8.0. Stepwise elution was used to wash away non-specifically bound proteins and elution of *Bli*Amy was achieved with 50 mM KPi buffer pH 8.0 containing 0.3 M imidazole. After SDS-PAGE analysis, fractions that contain the pure protein were pooled and the buffer was exchanged to 50 mM KPi, pH 6.5. The samples were flash frozen in liquid nitrogen and stored at -20 °C until use. Protein concentrations of purified *Bli*Amy and mutants were determined using the Bradford assay.

2.3 Crystallization, data collection, structure determination and refinement: Initial sitting-drop crystallization screening was performed using a Mosquito crystallization robot (TTP Labtech) in a 96-well MRC2 plate (Molecular Dimensions), with a protein concentration of 7.5 mg/mL in 50 mM HEPES (pH 7.5), 5 mM $CaCl_2$ and 150 mM NaCl. The screening solutions used for the experiments were PACT, Wizard and JCSG+ (Molecular Dimensions) and Index and Grid Screen Salt (Hampton). Bipyramidal crystals appeared after 1 week of incubation at 294 K in solutions containing malonate at pH 5 to 6. Crystallization conditions were optimized using sitting-drop set-ups with 42-46% (v/v) tacsimate (Hampton), containing 1.36 M malonic acid, 0.25 M ammonium citrate tribasic, 0.12 M succinic acid, 0.3 M D,L-malic acid, 0.4 M sodium acetate, 0.5 M sodium formate, 0.16 M ammonium tartrate dibasic at pH 6.0 and 10 mM $CaCl_2$, as precipitant. Drops contained 0.1 µL protein solution and 0.1 µL reservoir solution. Crystals grown from malonate or tacsimate without $CaCl_2$ showed worse morphology and did not diffract.

Before data collection, crystals were briefly soaked in a cryoprotectant solution consisting of 60% (v/v) tacsimate and 10 mM $CaCl_2$. Ligand complexes were obtained by soaking crystals in 25 mM acarbose (Tokyo Chemical Industry Co., Ltd.), a glycoside hydrolase inhibitor, and 100 mM maltose (ACR-MAL) for 20 min, 100 mM maltose (MAL), 100 mM maltohexaose (G6) or 20 mM β-cyclodextrin (β-CD) added to the cryoprotectant for a few min. X-ray diffraction data were collected on an in-house MarDTB Goniostat System using Cu-*Kα* radiation from a Bruker MicrostarH rotating-anode generator equipped with HeliosMX mirrors. Intensity data were processed using iMosflm [30].

*Bli*Amy crystals belong to the tetragonal space group $P4_32_11$ with one monomer of 55 kDa in the asymmetric unit. The V_M is 3.0 $Å^3$/Da [31] with a solvent content of 59%. Data collection statistics are listed in Table 1. The structure of the *Bli*Amy was determined by the molecular replacement method using Phaser [32] with mixed model coordinates of *B. licheniformis* alpha-amylase (BLA) [33] (PDB code:1BLI) as search model.

The model was refined with REFMAC5 [34] and Coot [35] was used for manual rebuilding and map inspection. Continuous density in 2*mFo-DFc* and *mFo - DFc* maps for two acarbose

molecules per protein molecule was observed in the ACR-MAL crystal, one bound in the active site and one bound at a remote location**.** In the secondary substrate binding site electron density is visible for four of the six sugar residues in the G6 experiment; maltose in the MAL experiment and β-cyclodextrin in the β-CD experiment. One TLS group was used in the last rounds of refinement. The quality of the models was analyzed with PDB_REDO [36] and MolProbity [37]. Atomic coordinates and experimental structure factor amplitudes have been deposited in the Protein Data Bank (PDB) (Table 1).

2.4 Strains, plasmids and site directed mutagenesis: The Agilent primer design tool (www.agilent.com) was used to design primers to create mutants F257A, Y358A and F257A/Y358A using QuikChange site-directed mutagenesis. Oligonucleotide sequences used for generation of mutants are available upon request. Two primers were used in each PCR reaction, using the *Pfu*Ultra II Master Mix (Agilent) as recommended by the supplier. The pBad-6xHis-*Bli*Amy construct was used as a template which results in expression of *Bli*Amy mutants with an N-terminal His tag. The pBad-6xHis-*Bli*Amy F257A construct was used as a template to introduce the Y358A mutation and thus generate the construct for expression of double mutant, pBad-6xHis-*Bli*Amy F257A/Y358A. Obtained constructs were transformed into chemically competent NEB10β cells. Plasmid sequences were verified by sequencing (GATC).

2.5 Kinetic studies with pNP-G6: The chromogenic substrate 4-nitrophenyl α-D-maltohexaoside (pNP-G6) was purchased from Merck (Kenilworth, NJ, United States). Determination of kinetic parameters of *Bli*Amy variants for pNP-G6 was monitored by the increase in absorbance at 405 nm using a Shimadzu UV spectrophotometer UV-1800. The concentration of enzyme used was 110 nM for all assays. All experiments were carried out in triplicate. Initial rates were measured using five to seven different pNP-G6 concentrations ranging from 0.05 to 5 mM in 100 mM Tris·HCl buffer, pH 8.0, at 25°C and fit to the Michaelis – Menten equation by nonlinear regression using GraphPad Prism 5 to obtain V_{max} (k_{cat}) and K_m.

2.6 Kinetic studies with soluble starch: Rates of enzymatic hydrolysis of soluble starch were determined by quantifying the concentration of sugar reducing ends using the DNS assay [38]. A stock solution (50 mg/mL) of soluble potato starch (Merck) was made in 50 mM phosphate buffer, pH 6.5. Starch solutions at various concentrations (0 to 42 mg/mL) were prepared by diluting with buffer. Purified *Bli*Amy variants (final concentration 75 nM) were added to starch solutions and incubated at 60°C for an appropriate length of time. The reactions were stopped by addition of an equal volume of DNS solution and the color was developed by boiling the samples for 5 min, followed by cooling at room temperature. The absorbance was measured spectrophotometrically at 540 nm and values were plotted versus reaction time. Maltose was used as a standard. All experiments were carried out in triplicate. The initial rates were plotted against substrate concentration and fitted to the Michaelis – Menten equation by nonlinear regression using GraphPad Prism 5 to obtain V_{max} (k_{cat}) and K_m.

2.7 Kinetic studies with starch granules: Purified *Bli*Amy variants (3 to 540 nM) were added to corn starch granules suspended at 10 concentrations (0 to 270 mg/mL) in 50 mM

phosphate buffer, pH 6.5, and 0.005% (w/v) BSA. All experiments were carried out in triplicate. After incubation at 60°C for 1 h reducing sugars were measured in supernatants after centrifugation (16,000*g* for 3 min). Catalytic coefficients (k_{cat}/K_m) for all variants were obtained from the slopes of v_i/[E] versus [S], where v_i represents initial rates [14], using GraphPad Prism 5.

2.8 Starch granules adsorption assays: Purified *Bli*Amy variants (16 nM) and corn starch granules at 10 concentrations (0 – 100 mg/mL) in 50 mM phosphate buffer, pH 6.5, and 0.005% (w/v) BSA were incubated in triplicate at 4°C for 30 min with continuous shaking at 300 rpm and centrifuged (16,000*g* and 4°C for 15 min) [14]. Enzyme remaining in the supernatants was assayed by measuring activity toward soluble starch and expressed as the percentage of bound enzyme when compared with a no-starch control. No-starch control was also confirmation that the stability of the active enzyme was completely retained in the starch granule binding assays under the experimental conditions used. Values were plotted against the starch concentrations, and the data were fitted to a one-site binding model using GraphPad Prism 5. The dissociation constant K_d was obtained by fitting the Langmuir adsorption isotherm to the fraction of bound enzyme (eq 1) *B* being the bound enzyme fraction, [S] the starch granule concentration, and B_{max} the maximum binding capacity [14].

$$B = \frac{B_{max}\,[S]}{K_d + [S]} \qquad (1)$$

3. RESULTS AND DISSCUSION

3.1 The crystal structure of *Bli*Amy

The crystal structure of *Bacillus paralicheniformis* strain ATCC 9945a amylase was determined with molecular replacement to 1.95 Å resolution. The structure consists of three domains. The N-terminal catalytic domain A, comprising 291 residues (3 to 103 and 206 to 396), forms a $(\beta/\alpha)_8$-barrel structure. Domain B (residues 104-206) is inserted between the third β-strand and the third α-helix of domain A and consists of two extended loops. The C-terminal domain C (residues 397-482) folds into an eight-stranded antiparallel β-barrel (Fig. 1).

The structure of the *Bli*Amy is similar to that of amylases from *Bacillus licheniformis* (BLA). The sequence of *Bli*Amy is 96% identical to the calcium-free wild-type BLA (PDB code 1VJS, 0.46 Å rmsd) [39] which is identical to PDB 1BPL (0.62Å rmsd) [40]. *Bli*Amy is 95% identical to a calcium-containing variant BLA (PDB 1BLI, 0.43 Å rmsd) [33] and a thermostabilized α-amylase (PDB 1OB0, 0.79Å rmsd) [41].

In the *Bli*Amy structure, the Ca-Na-Ca metal triad, necessary for structural integrity and enzymatic activity [33], is situated between domains A and B (Fig. 1), and is identical to that in the Ca^{2+}-containing BLA (1BLI). A Na^+ ion in the structure of *Bli*Amy is replacing the third Ca^{2+} ion between domains A and C (Fig. 2 A-D). The anomalous difference Fourier map did not confirm a

Ca^{2+} ion at this location. The ligands for this Na^{+} ion are G300-O (2.5 Å), Y302-O (2.1 Å), H406-O (2.6 Å), H406-ND1 (3.3 Å), N407 OD1 (2.4 Å), and D430-OD1 and OD2 (both 2.5 Å). A Cl^{-} ion reported for some other structures was also not visible in the anomalous map [40]. The *cis* peptide bond between W184 and E185 is vital for maintaining the integrity of the cage surrounding the Ca-Na-Ca metals [33]. In the native structure of *Bli*Amy W184 is observed with two diverse side chain conformations while in the acarbose soak the tryptophan shows a third conformation. The different conformations are probably due to crystal contacts. In the native structure the tryptophan in both conformations has cation-π interaction with the symmetry related R93 and in the acarbose structure the W-NE1 has a hydrogen bond with the symmetry related D94-OD2. In the other determined structures, multiple conformations for W184 are also observed.

The active site of *Bli*Amy is located in a large cleft at the C-terminal end of the $(\beta/\alpha)_8$-barrel of domain A and is identical to the active site in the above-mentioned structures. In the native structure a malonate molecule from the crystallization medium is bound in the active site. It is hydrogen bonded to H235 (+1 sugar subsite) and E261-OE2, which exhibits a double conformation.

3.2 Crystal structures of *Bli*Amy in complex with oligosaccharides and oligosaccharide precursors

The crystal structure of *Bli*Amy in complex with acarbose (ACR-MAL) revealed that *Bli*Amy binds two acarbose molecules, one in the active site, i.e. at the C-terminal end of the $(\beta/\alpha)_8$-barrel (Fig. 1) and one at the N-terminal end (Fig. 2A). The acarbose molecule in the active site is bound in subsites -1 to +3, spanning the cleavage point at -1/+1. The enzyme utilizes a retaining mechanism with D231, E261, and D328 involved as catalytic residues. This acarbose has similar interactions to the enzyme as described by Davies et al. for *B. halmapalus* α-amylase (BHA) [42].

At the +1 binding site, the acid/base catalyst E261-OE2 has hydrogen bond interactions (2.8 Å) with the NH group of the valienamine of the acarbose. The proton donor D328 (OD2) has interaction with the NH group (3.1 Å) and O2 of the valienamine (2.6 Å) as well as between D328 (OD1) and O3 of the valienamine (2.8 Å). Other interactions are between H327 (NE2) and both O2 and O3 of the valienamine (both 2.9 Å), between H105 and D231 and O6 and between R229-NH1 and O2. Stacking interaction is observed of the valienamine ring and Y56. At the -1 binding site E261-OE1 has interaction with O3 and H235-NE2 with O2. At the +2 binding site K234-NZ has interaction with O3 and O2, and E189-OE1 and OE2 have interaction with O2. At the +3 binding site stacking interaction with Y290 is observed. Because of steric hindrance by a symmetry related molecule in the crystal structure binding of a sugar molecule at the -2 binding site is not possible.

The remotely bound acarbose molecule is situated at the bottom of the $(\beta/\alpha)_8$-barrel A domain at the other side of where the active site is located at a distance of ~35 Å (Fig. 2A). Its valienamine moiety has hydrogen bonds with T38-OG1, E255OE1 and OE2, and Y358-OH. Interactions of the protein with the dideoxy-glucose unit are of mainly hydrophobic nature. The sugar ring stacks on Y358 and with a T-shaped character on F257. One hydrogen bond is present to

the main-chain carbonyl atom of V318. The maltose moiety of the acarbose has hydrogen bond interactions with the amide backbone of G357, E355 OE1 and the backbone carbonyl of P317.

*Bli*Amy complexed with maltose (MAL) showed electron density for a disaccharide in the remote binding site (Fig. 2B). The two glucose units overlap with the acarviosin moiety of the acarbose and have similar contacts. The 6-hydroxyl of the maltose, absent in the dideoxy moiety, has backbone amide interaction with G5. A hydrogen bond is observed between the O5 of the glucose unit, located at the position of the cyclohexitol unit of acarbose, and the hydroxyl of Y98. This bond is absent in the *Bli*Amy acarbose complex as in cyclohexitol the oxygen atom is substituted by a carbon atom.

Furthermore, β-cyclodextrin (β-CD), the substrate analogue, is also bound only at the remote binding site (Fig. 2C). Of the seven glucose units in the ring, two overlap with the 2 glucose units of acarbose. They have similar interactions with the protein. Other interactions are of O2 and O3 with NZ of K319. On the other side O2 has interaction with E355-OE1. V318 binds to the hydrophobic cavity inside the β-CD.

The crystal soaked with maltohexaose (G6) showed electron density for a maltotetraose in the remote binding the site (Fig. 2D). The 2nd and 3rd glucose units overlap with the maltose and have similar interactions to the protein. The non-reducing end sugar (glucose-1) has only hydrogen bond interaction via O6 to backbone carbonyls of D94 and T38. The reducing end sugar (glucose-4) overlaps with the first glucose unit of the acarbose and has the same interaction to the protein. The outer 2 glucose units are probably flexible, not showing interactions with the protein and are therefore not visible in electron density. No conformational changes have been observed in the structure of *Bli*amy upon binding of the oligosaccharides or oligosaccharide precursors. The active sites of the crystals soaked with maltose, β-cyclodextrin and maltohexaose contain malonate, as in the native structure.

In conclusion, the crystallographic studies performed on *Bli*Amy with oligosaccharides or oligosaccharide precursors soaked into crystals of *Bli*Amy revealed one SBS with two key amino acids F257 and Y358 involved in binding (Fig. 2A-D)), providing a hydrophobic platform for the carbohydrates. The PDB entries for each structure obtained are provided in Table 1.

3.3 Presence of the *Bli*Amy SBS in other GH13_5 amylases

Glycoside hydrolase family 13 subfamily 5 (GH13_5), enclosing *Bli*Amy, contains structures of ten different sources of which five have saccharide binding at a region corresponding to the remote SBS observed in *Bli*Amy (Table 2 and 3). The chimeric amylase BA2, consisting of residues 1-300 from *B. amyloliquefaciens* and 301-483 from *B. licheniformis* has a maltotriose bound (PDB 1E40) (10 mM soak) which overlaps with glucose residues 1 to 3 of the tetraose in *Bli*Amy [43]. The maltotriose molecule observed at the SBS in *Bacillus* sp. 707 (AmyG6) [44] (PDB 2D3N) overlaps with glucose residues 2 to 4 of the *Bli*Amy tetraose structure. In the crystal structure of *B. stearothermophilus* STB04 (Bst-MFA) an acarbose molecule is bound at the SBS [45] (PDB code 6AG0) and has hydrophobic interactions with F4 (L3 in *Bli*Amy). This acarbose

molecule is shifted 2 glucose units to the N-terminus of the enzyme compared to the acarbose and by one glucose unit compared to the tetraose in *Bli*Amy. BHA [46] and *Alicyclobacillus* sp. 18711 (AliC) [47] amylases have a glucose molecule bound near the ring of a tyrosine corresponding to Y358 (in *Bli*Amy), which is an absolutely conserved residue in GH13_5 (Table 3). All ligands discussed have stacking interactions with Y358. Furthermore, an α-amylase from *Pyrococcus woesei* (PWA), a GH13_7 member (33% identity to *Bli*Amy), has several SBSs [48] (PDB 1MXD & 1MXG) of which one is similar to *Bli*Amy SBS. In PWA an acarbose molecule is interacting through hydrogen bonds and hydrophobic contacts with F279 (V318 in *Bli*Amy). The F257/Y358 pair of *Bli*Amy is lacking in PWA and other residues involved in the SBS are different (Table 3). The unpublished structure of PWA (PDB 3QGV) contains a β-cyclodextrin which overlaps with the β-CD at the SBS of *Bli*Amy.

The structural comparisons show that whereas the crystallographic studies have been done with different ligands and often with high ligand concentrations, corresponding oligosaccharide binding regions are visible in multiple amylase structures suggesting these are genuine SBSs and serve a biological function. The conservation of SBS residues at the subfamily level tends to be quite high, suggesting a similar function as for starch binding domains.

3.4 Other surface binding sites in GH13_5 glycosidases

In GH13_5 glycosidases, six surface binding sites distinct from the SBS found in *Bli*Amy are observed. A major docking platform is present in amylases AmyG6 (PDB 2D3N) [44, 59], BHA (2GJP) [46], AliC (6GXV) [47], *Halothermothrix orenii* (AmyB, PDB 3BC9) [63] (69, 72, 64 and 44% seq, identity respectively) and in other enzymes mentioned in Table 2 with involvement of two conserved tryptophan residues (W138/W165 in *Bli*Amy). In AmyG6 W140 and W167 stack with the glucose molecules at subsites -5 and -6 of the active site (Fig. 3A) [59]. W140 is located 24 Å away from the active site but plays a critical role in binding and hydrolyzing amylose [44]. This SBS is not accessible in the crystal structure of *Bli*Amy as a result of crystal packing contacts. W165 of *Bli*Amy has π-π interactions with W165 from a symmetry related molecule and W138 has hydrophobic interactions with the side chain of K70 from the same symmetry related molecule. AliC (PDB code 6GXV, 64 % seq. identity) has a similar 3-domain structure and an SBS near another conserved tryptophan of the $(\beta/\alpha)_8$ barrel domain (Fig. 3B) [47]. However, in *Bli*Amy W184, required for the integrity of the metal binding cage, is also involved in crystal contacts with an arginine side chain of a symmetry related molecule and this site is therefore not available for saccharide binding. Another residue involved in crystal contacts is the conserved W342 of *Bli*Amy. A maltose molecule is stacked on that tryptophan residue in BHA (Fig. 3C) (PDB 2GJP) [46], Bst-MFA (PDB 6AG0) [45] and AmyG6 (PDB 2D3N) (72, 66 and 69% seq. identity respectively). W138/W165, W184 and W342 are involved in crystal contacts, artifacts of crystallization, and are not available as SBSs. Nevertheless, these SBSs will probably be accessible in *Bli*Amy in solution.

Another SBS is observed in BHA (PDB 2GJP, 66% seq. identity) in which a glucose molecule stacks on the platform of W439/W469 (Fig. 3D) [46]. *Bli*Amy contains R437/W467 at the

corresponding positions. Having just one tryptophan residue probable lowers the affinity for saccharides as no binding was observed at this position in *Bli*Amy. Additionally, AmyG6 (69% seq. identity) has a glucose/maltose binding site near another tryptophan (Fig. 3E) [44] (PDB 2D3L/2D3N). The corresponding F279 of *Bli*Amy shows no sugar binding. A further SBS is observed in Bst-MFA (PDB 6AG0, 66% seq. identity) near the conserved Y159 (Fig. 3F), here also no binding is observed in *Bli*Amy.

In summary, *Bli*Amy probably has additional sugar binding sites at W138/W165, W184 and W342 but sugar binding is not observed in our structures since these residues are involved in crystal formation. The other tryptophan residues are located inside the enzyme or are not oriented in a parallel manner at the surface.

3.5 SBSs in other GH13 amylases

Many amylases, such as barley α-amylase GH13_6 [49], human salivary amylase GH13_24 [15], and pig pancreatic amylase GH13_24 [50] do not have a starch-binding CBM, but instead have one or more SBSs on the catalytic domain that enable raw starch utilization [16]. At these domains, aromatic amino acids play an important role in hydrophobic stacking interactions to carbohydrates complemented with hydrogen bonds [19].

Common SBSs architectures include two spatially locked aromatic residues, such as SBS1 (starch granule binding site) in barley α-amylase (PDB 2QPU) comprised of W278 and W279 (Fig. 4A) [14, 49], SBS1 is absent *in Bli*Amy which has a lysine and histidine at that location. The other sites in *Bli*Amy involving tryptophans are blocked by crystal contacts as described above. Several other amylases contain such an SBS consisting of the two aromatic planes with an angle of 130° between them that thereby form an arc parallel to the surface of enzyme [19]. It is proposed that this arc is complementary to the natural helical twist of α-glucan chains in many substrates, including starch, so their probable function is to act as initial starch recognition platform [14, 16, 49, 51]. SBS1-like motifs have been seen in other amylolytic enzymes such as Y276/W284 in porcine pancreatic *α*-amylase [52] and SBS7 in human pancreatic *α*-amylase [17] involved with the raw starch hydrolysis which also have a form of a platform that matches the lower faces of the sugar rings in the bound structure. Y276/W284 was also found in human salivary *α*-amylase [15] and W439/W469 in BHA (see above) [46], suggesting these sites perform similar functions in their respective enzymes as described for barley α-amylase [49].

Another example of an SBS architecture is SBS2 (pair of sugar tongs binding site) in barley α-amylase [49] with two aromatic residues, Y380 and H395 (Fig. 4B) located on the C-domain. This type of interaction has been termed as “tweezers” since the site can bind accessible α-glucan chains and position them correctly in the active site [14, 19, 49, 51]. *Bli*Amy does not have the SBS2, instead G433 in *Bli*Amy is located at the position of Y380, while a loop with residues T453 - N455 is situated at the position of H395.

SusG utilizes the architecture of an aromatic platform including W460 and Y469 of the A domain as SBS [16] (Fig. 4C, Table 2). The placement of the SBS adjacent to the active site is unique, whereas these SBSs in other amylases are typically separated by distances of 15 Å or more [16]. Further, in SusG, the reducing ends of the bound oligosaccharides are pointed toward each other, making it unlikely that a single α-glucan chain spans both sites, which led authors to suggest that the role of this SBS is in retaining reaction products for subsequent passage to other proteins of the starch utilization system [16].

In GH13_28 amylase from *Bacillus subtilis* 2633 [53] and GH13_32 amylase from *Alteromonas haloplanctis* [54] complexes with acarbose in the active site were observed, however SBSs were not detected.

None of the architectures described in this section above correspond to the SBS found in this work. The two most determinant residues are Y358 and F257 which show edge-to-face π-π interaction with each other. The rings of F257 and Y98 show parallel displaced π-π interaction. These three residues form a platform for carbohydrate binding in which only Y358 has stacking interaction with the carbohydrate. This SBS was first observed in BHA [46] but was not further characterized.

3.6 Biochemical characterization of *Bli*Amy surface binding site

To understand the possible role of SBS in *Bli*Amy, the two most important amino acids were mutated both individually and simultaneously to obtain variants F257A, Y358A and F257A/Y358A. This approach was aimed at removing the hydrophobic stacking interactions with carbohydrates observed in the crystal structure with β-cyclodextrin and other oligosaccharides mentioned above. Mutagenesis is an effective tool for eliminating binding at SBS sites which allows evaluation of the impact on activity and binding characteristics, as shown in several cases of different amylases [14, 16, 17, 55].

Kinetic parameters for hydrolysis of the amylase substrate pNP-G6 [56] were first determined for each variant protein and wild type *Bli*Amy and are listed in Table 4, as a confirmation of the integrity of the active site [17]. All variants show almost the same k_{cat}/K_m values indicating that they had all folded into the catalytically active form, i.e. binding at the active site was not significantly affected by structural changes at remote surface site. A similar outcome was observed for human pancreatic α-amylase SBSs [17].

Kinetic parameters for hydrolysis of the soluble starch were determined for each variant protein and WT *Bli*Amy and are listed in Table 4. The hydrolysis efficiency of soluble starch by the double mutant was slightly compromised since the double mutant showed a decrease of k_{cat}/K_m to 47% as compared to the wild type (Table 4), while mutating only one of the two SBS residues (Y358A or F257A) did not affect $k_{cat.}$ However, a 2-fold reduction of the k_{cat} of F257A/Y358A mutant suggests possible impact of the SBS in formation of productive complexes between enzyme and longer α-glucan chains.

For all SBS mutants and WT, like in the work of Nielsen et al. [14], only the catalytic efficiency (k_{cat}/K_m) and not the individual k_{cat} and K_m values for hydrolysis of raw starch granules could be determined. The results obtained (Table 4, Fig. 5) suggest that the hydrolysis of raw starch is affected by both F257A and Y358A mutations, both showing ~50% reduction in catalytic efficiency. For the F257A/Y358A mutant we can observe additive effect on catalytic efficiency. The double mutant had 5-fold lower efficacy with corn starch as a substrate compared to WT *Bli*Amy, suggesting that both amino acids F257 and Y358 play a role in processing of an insoluble α-glucan (Table 4, Fig. 5).

The ability of *Bli*Amy and its variants to get adsorbed to the raw corn starch was investigated to establish the role of F257 and Y358 as a surface binding site for starch. A commonly employed assay for the binding of enzymes to starch granule shows that in *Bli*Amy mutation of SBS at F257A and Y358A led to a 1.6- and 3.5-fold reduction in affinity for starch granules, respectively (Fig. 6, values obtained from eq. 1). Mutation of both sites (F257A/Y358A) results in at least 5.5-fold weaker binding compared to the WT (apparent K_d values, Fig. 6). Increase in apparent K_d along with the significant drop in starch saturation binding level B_{max} for the double mutant confirms that SBS enhances the ability of *Bli*Amy to bind insoluble corn starch. F257 and Y358 each contributed cumulatively to ensure optimal binding to the starch granule, although having just one tyrosine for stacking (and hydrogen bonds and Van der Waals interactions).

The functional relevance of SBSs in several α-amylases was investigated by mutational analysis. The SusG mutant constructed by mutating the SBS (W460A/Y469A/D473V) showed up to 56% decrease in activity when tested for raw corn starch hydrolysis [16], while seriously diminished binding of a mutant at SBS (Y276A/W284A) to starch granules was observed for human pancreatic amylase [17]. The complete loss of affinity for barley starch granules was found when both SBSs were mutated (W278A/W279A/Y380A) at the same time and it retained only 0.2% of the wild type hydrolytic activity for barley starch granules [14]. For a 6-fold mutant involving four SBSs of human salivary α-amylase the specific activity for starch hydrolysis resulted in a significant reduction in enzyme activity (10-fold) compared to wild type enzyme [15]. At the same time the raw starch-binding ability of wild type enzyme was 91% and for the mutant only 13%.

4. Conclusions

An unusual starch binding site was found in a groove on the surface of the *Bli*Amy protein. Significance of the starch binding site was verified by mutational analysis of two key amino acids F257 and Y358. Removal of the aromatic residues in the SBS led to weaker raw starch binding and raw starch-hydrolyzing activity, confirming that the SBS is an important site in α-amylases for increasing raw starch digestibility. This SBS may support the identification of potential SBSs in other GH13_5 amylases due to quite high conservation of SBS residues at the subfamily level or in similar enzymes from other subfamilies within the *α*-amylase family GH13 despite the lack of sequence conservation.

Acknowledgments:

Author Contributions: Conceptualization, N.B., H.J.R.; methodology, N.B., H.J.R., M.S.S.; investigation, N.B., H.J.R., N.L.; protein crystallography and structure analysis, H.J.R., resources, D.B.J. and Z.V.; writing—original draft preparation, N.B., H.J. R.; writing—review and editing, all authors.

Funding: This work was financially supported by the Ministry of Education, Science and Technological Development of Republic of Serbia Contract numbers: 451-03-68/2020-14/200168 and 451-03-68/2020-14/200026

Conflicts of Interest: The authors declare no conflict of interest.

Journal Pre-proof

REFERENCES

[1] N. Karaki, A. Aljawish, C. Humeau, L. Muniglia, J. Jasniewski, Enzymatic modification of polysaccharides: Mechanisms, properties, and potential applications: A review, Enzyme Microb. Technol. 90 (2016) 1-18, https://doi.org/10.1016/j.enzmictec.2016.04.004.

[2] V. Vamadevan, E. Bertoft, Structure-function relationships of starch components, Starch-Starke 67(1-2) (2015) 55-68, https://doi.org/10.1002/star.201400188.

[3] J. Tan, C. McKenzie, M. Potamitis, A.N. Thorburn, C.R. Mackay, L. Macia, The role of short-chain fatty acids in health and disease, Adv. Immunol. 121 (2014) 91-119, https://doi.org/10.1016/B978-0-12-800100-4.00003-9.

[4] G.H. Robertson, D.W.S. Wong, C.C. Lee, K. Wagschal, M.R. Smith, W.J. Orts, Native or raw starch digestion: A key step in energy efficient biorefining of grain, J. Agric. Food Chem. 54(2) (2006) 353-365, https://doi.org/10.1021/Jf051883m.

[5] U. Uthumporn, I.S.M. Zaidul, A.A. Karim, Hydrolysis of granular starch at sub-gelatinization temperature using a mixture of amylolytic enzymes, Food Bioprod. Process. 88(C1) (2010) 47-54, https://doi.org/10.1016/j.fbp.2009.10.001.

[6] B.A. Cinelli, L.R. Castilho, D.M.G. Freire, A.M. Castro, A brief review on the emerging technology of ethanol production by cold hydrolysis of raw starch, Fuel 150 (2015) 721-729, https://doi.org/10.1186/s13068-016-0636-5.

[7] N. Božić, N. Lončar, M. Šokarda Slavić, Z. Vujčić, Raw starch degrading α-amylases: an unsolved riddle, Amylase 1 (2017) 12-25, https://doi.org/10.1515/amylase-2017-0002.

[8] A.B. Boraston, D.N. Bolam, H.J. Gilbert, G.J. Davies, Carbohydrate-binding modules: fine-tuning polysaccharide recognition, Biochem. J. 382(Pt 3) (2004) 769-781, https://doi.org/10.1042/BJ20040892.

[9] H. Hashimoto, Recent structural studies of carbohydrate-binding modules, Cell Mol. Life Sci. 63(24) (2006) 2954-2967, https://doi.org/10.1007/s00018-006-6195-3.

[10] S. Armenta, S. Moreno-Mendieta, Z. Sanchez-Cuapio, S. Sanchez, R. Rodriguez-Sanoja, Advances in molecular engineering of carbohydrate-binding modules, Proteins 85(9) (2017) 1602-1617, https://doi.org/10.1002/prot.25327.

[11] H.J. Gilbert, J.P. Knox, A.B. Boraston, Advances in understanding the molecular basis of plant cell wall polysaccharide recognition by carbohydrate-binding modules, Curr. Opin. Struct. Biol. 23(5) (2013) 669-677, https://doi.org/10.1016/j.sbi.2013.05.005.

[12] Š. Janeček, F. Mareček, E.A. MacGregor, B. Svensson, Starch-binding domains as CBM families-history, occurrence, structure, function and evolution, Biotechnol. Adv. 37(8) (2019) p. 107451, https://doi.org/10.1016/j.biotechadv.2019.107451.

[13] D. Cockburn, C. Wilkens, A. Dilokpimol, H. Nakai, A. Lewinska, M. Abou Hachem, B. Svensson, 2016. Using carbohydrate interaction assays to reveal novel binding sites in carbohydrate active enzymes. PLOS One. 11(8), e0160112. https://doi.org/10.1371/journal.pone.0160112.

[14] M.M. Nielsen, S. Bozonnet, E.S. Seo, J.A. Motyan, J.M. Andersen, A. Dilokpimol, M. Abou Hachem, G. Gyemant, H. Naested, L. Kandra, B.W. Sigurskjold, B. Svensson, Two secondary carbohydrate binding sites on the surface of barley α-amylase 1 have distinct functions and display synergy in hydrolysis of starch granules, Biochemistry 48(32) (2009) 7686-7697, https://doi.org/10.1021/bi900795a.

[15] C. Ragunath, S.G. Manuel, V. Venkataraman, H.B. Sait, C. Kasinathan, N. Ramasubbu, Probing the role of aromatic residues at the secondary saccharide-binding sites of human salivary α-amylase in substrate hydrolysis and bacterial binding, J. Mol. Biol. 384(5) (2008) 1232-1248, https://doi.org/10.1016/j.jmb.2008.09.089.

[16] N.M. Koropatkin, T.J. Smith, SusG: a unique cell-membrane-associated α-amylase from a prominent human gut symbiont targets complex starch molecules, Structure 18(2) (2010) 200-215, https://doi.org/10.1016/j.str.2009.12.010.

[17] X.H. Zhang, S. Caner, E. Kwan, C.M. Li, G.D. Brayer, S.G. Withers, Evaluation of the significance of starch surface binding sites on human pancreatic α-amylase, Biochemistry 55(43) (2016) 6000-6009, https://doi.org/10.1021/acs.biochem.6b00992.

[18] D. Cockburn, C. Wilkens, C. Ruzanski, S. Andersen, J.W. Nielsen, A.M. Smith, R.A. Field, M. Willemoes, M. Abou Hachem, B. Svensson, Analysis of surface binding sites (SBSs) in carbohydrate active enzymes with focus on glycoside hydrolase families 13 and 77-a mini-review, Biologia 69(6) (2014) 705-712, https://doi.org/10.2478/s11756-014-0373-9.

[19] S. Cuyvers, E. Dornez, J.A. Delcour, C.M. Courtin, Occurrence and functional significance of secondary carbohydrate binding sites in glycoside hydrolases, Crit. Rev. Biotechnol. 32(2) (2012) 93-107, https://doi.org/10.3109/07388551.2011.561537.

[20] D. Cockburn, B. Svensson, Structure and functional roles of surface binding sites in amylolytic enzymes, in: A. Svendsen (Ed.), Understanding Enzymes, Function, design, engineering and analysis, Pan Stanford Publishing Pte. Ltd. 2016, pp. 267-295.

[21] U. Baroroh, M. Yusuf, S.D. Rachman, S. Ishmayana, M. Syamsunarno, J. Levita, T. Subroto, 2017. The importance of surface-binding site towards starch-adsorptivity level in α-amylase: A review on structural point of view. Enzyme Res. 2017, 4086845. https://doi.org/10.1155/2017/4086845.

[22] N. Božić, J.-M. Puertas, N. Lončar, C. Sans Duran, J. López-Santín, Z. Vujčić, The DsbA signal peptide-mediated secretion of a highly efficient raw-starch-digesting, recombinant α-amylase from *Bacillus licheniformis* ATCC 9945a, Process Biochem. 48(3) (2013) 438-442, https://doi.org/10.1016/j.procbio.2013.01.016.

[23] M. Šokarda Slavić, M. Pešić, Z. Vujčić, N. Božić, Overcoming hydrolysis of raw corn starch under industrial conditions with *Bacillus licheniformis* ATCC 9945a α-amylase, Appl. Microbiol. Biotechnol. 100(6) (2016) 2709–2719, https://doi.org/10.1007/s00253-015-7101-4.

[24] G. Tawil, A. Vikso-Nielsen, A. Rolland-Sabate, P. Colonna, A. Buleon, Hydrolysis of concentrated raw starch: A new very efficient α-amylase from *Anoxybacillus flavothermus*, Carbohyd. Polym. 87(1) (2012) 46-52, https://doi.org/10.1016/j.carbpol.2011.07.005.

[25] D. Mehta, T. Satyanarayana, Domain C of thermostable α-amylase of *Geobacillus thermoleovorans* mediates raw starch adsorption, Appl. Microbiol. Biotechnol. 98(10) (2014) 4503-4519, https://doi.org/10.1007/s00253-013-5459-8.

[26] A. Vikso-Nielsen, C. Andersen, T. Hoff, S. Pedersen, Development of new α-amylases for raw starch hydrolysis, Biocatal. Biotransfor. 24(1-2) (2006) 121-127, https://doi.org/10.1080/10242420500519191.

[27] M.J. van der Maarel, B. van der Veen, J.C. Uitdehaag, H. Leemhuis, L. Dijkhuizen, Properties and applications of starch-converting enzymes of the α-amylase family, J. Biotechnol. 94(2) (2002) 137-155, https://doi.org/10.1016/s0168-1656(01)00407-2.

[28] S. Janecek, B. Svensson, E.A. MacGregor, α-Amylase: an enzyme specificity found in various families of glycoside hydrolases, Cell Mol. Life Sci. 71(7) (2014) 1149-1170, https://doi.org/10.1007/s00018-013-1388-z.

[29] N. Lončar, M. Šokarda Slavić, Z. Vujčić, N. Božić, 2015. Mixed-mode resins: taking shortcut in downstream processing of raw-starch digesting α-amylases, Sci. Rep. 5, 15772. https://doi.org/10.1038/srep15772.

[30] H.R. Powell, O. Johnson, A.G.W. Leslie, Autoindexing diffraction images with iMosflm, Acta Cryst. D. 69 (2013) 1195-1203, https://doi.org/10.1107/S0907444912048524.

[31] B.W. Matthews, Solvent content of protein crystals, J. Mol. Biol. 33(2) (1968) 491-497, https://doi.org/10.1016/0022-2836(68)90205-2.

[32] A.J. Mccoy, R.W. Grosse-Kunstleve, P.D. Adams, M.D. Winn, L.C. Storoni, R.J. Read, Phaser crystallographic software, J. Appl. Cryst. 40 (2007) 658-674, https://doi.org/10.1107/S0021889807021206.

[33] M. Machius, N. Declerck, R. Huber, G. Wiegand, Activation of *Bacillus licheniformis* alpha-amylase through a disorder -> order transition of the substrate-binding site mediated by a calcium-sodium-calcium metal triad, Structure 6(3) (1998) 281-292, https://doi.org/10.1016/s0969-2126(98)00032-x.

[34] M.D. Winn, C.C. Ballard, K.D. Cowtan, E.J. Dodson, P. Emsley, P.R. Evans, R.M. Keegan, E.B. Krissinel, A.G. Leslie, A. McCoy, S.J. McNicholas, G.N. Murshudov, N.S. Pannu, E.A. Potterton, H.R. Powell, R.J. Read, A. Vagin, K.S. Wilson, Overview of the CCP4 suite and current developments, Acta Cryst. D. 67(Pt 4) (2011) 235-242, https://doi.org/10.1107/S0907444910045749.

[35] P. Emsley, B. Lohkamp, W.G. Scott, K. Cowtan, Features and development of Coot, Acta Cryst. D. 66(Pt 4) (2010) 486-501, https://doi.org/10.1107/S0907444910007493.

[36] R.P. Joosten, F. Long, G.N. Murshudov, A. Perrakis, The PDB_REDO server for macromolecular structure model optimization, IUCrJ 1(Pt 4) (2014) 213-220, https://doi.org/10.1107/S2052252514009324.

[37] V.B. Chen, W.B. Arendall 3rd, J.J. Headd, D.A. Keedy, R.M. Immormino, G.J. Kapral, L.W. Murray, J.S. Richardson, D.C. Richardson, MolProbity: all-atom structure validation for macromolecular crystallography, Acta Cryst. D. 66(Pt 1) (2010) 12-21, https://doi.org/10.1107/S0907444909042073.

[38] P. Bernfeld, Amylases, α and β, in: P. De Murray (Ed.), Methods in enzymology, Deutcher Academic Press INC, San Diego, California, 1955, pp. 149-158.

[39] K.Y. Hwang, H.K. Song, C. Chang, J. Lee, S.Y. Lee, K.K. Kim, S. Choe, R.M. Sweet, S.W. Suh, Crystal structure of thermostable α-amylase from *Bacillus licheniformis* refined at 1.7 angstrom resolution, Mol. Cells 7(2) (1997) 251-258.

[40] M. Machius, G. Wiegand, R. Huber, Crystal structure of calcium-depleted *Bacillus licheniformis* α-amylase at 2.2 A resolution, J. Mol. Biol. 246(4) (1995) 545-559, https://doi.org/10.1006/jmbi.1994.0106.

[41] M. Machius, N. Declerck, R. Huber, G. Wiegand, Kinetic stabilization of *Bacillus licheniformis* α-amylase through introduction of hydrophobic residues at the surface, J. Biol. Chem. 278(13) (2003) 11546-11553, https://doi.org/10.1074/jbc.M212618200.

[42] G.J. Davies, A.M. Brzozowski, Z. Dauter, M.D. Rasmussen, T.V. Borchert, K.S. Wilson, Structure of a *Bacillus halmapalus* family 13 α-amylase, BHA, in complex with an acarbose-derived nonasaccharide at 2.1 angstrom resolution, Acta Cryst. D. 61 (2005) 190-193, https://doi.org/10.1107/S0907444904027118.

[43] A.M. Brzozowski, D.M. Lawson, J.P. Turkenburg, H. Bisgaard-Frantzen, A. Svendsen, T.V. Borchert, Z. Dauter, K.S. Wilson, G.J. Davies, Structural analysis of a chimeric bacterial α-amylase. High-resolution analysis of native and ligand complexes, Biochemistry 39(31) (2000) 9099-9107, https://doi.org/10.1021/bi0000317.

[44] R. Kanai, K. Haga, T. Akiba, K. Yamane, K. Harata, Role of Trp140 at subsite-6 on the maltohexaose production of maltohexaose-producing amylase from alkalophilic *Bacillus* sp.707, Prot. Sci. 15(3) (2006) 468-477, https://doi.org/10.1110/Ps.051877006.

[45] X. Xie, Y. Li, X. Ban, Z. Zhang, Z. Gu, C. Li, Y. Hong, L. Cheng, T. Jin, Z. Li, Crystal structure of a maltooligosaccharide-forming amylase from *Bacillus stearothermophilus* STB04, Int. J. Biol. Macromol. 138 (2019) 394-402, https://doi.org/10.1016/j.ijbiomac.2019.07.104.

[46] L. Lyhne-Iversen, T.J. Hobley, S.G. Kaasgaard, P. Harris, Structure of *Bacillus halmapalus* α-amylase crystallized with and without the substrate analogue acarbose and maltose, Acta Cryst. F. 62 (2006) 849-854, https://doi.org/10.1107/S174430910603096x.

[47] J. Agirre, O. Moroz, S. Meier, J. Brask, A. Munch, T. Hoff, C. Andersen, K.S. Wilson, G.J. Davies, The structure of the AliC GH13 α-amylase from *Alicyclobacillus* sp. reveals the

accommodation of starch branching points in the α-amylase family, Acta Cryst. D. 75(Pt 1) (2019) 1-7, https://doi.org/10.1107/S2059798318014900.

[48] A. Linden, O. Mayans, W. Meyer-Klaucke, G. Antranikian, M. Wilmanns, Differential regulation of a hyperthermophilic α-amylase with a novel (Ca,Zn) two-metal center by zinc, J. Biol. Chem. 278(11) (2003) 9875-9884, https://doi.org/10.1074/jbc.M211339200.

[49] X. Robert, R. Haser, H. Mori, B. Svensson, N. Aghajari, Oligosaccharide binding to barley α-amylase 1, J. Biol. Chem. 280(38) (2005) 32968-32978, https://doi.org/10.1074/jbc.M505515200.

[50] M. Qian, R. Haser, F. Payan, Carbohydrate binding sites in a pancreatic α-amylase-substrate complex, derived from X-ray structure analysis at 2.1 A resolution, Protein Sci. 4(4) (1995) 747-755, https://doi.org/10.1002/pro.5560040414.

[51] K. Sorimachi, M.F. Le Gal-Coeffet, G. Williamson, D.B. Archer, M.P. Williamson, Solution structure of the granular starch binding domain of *Aspergillus niger* glucoamylase bound to β-cyclodextrin, Structure 5(5) (1997) 647-661, https://doi.org/10.1016/s0969-2126(97)00220-7.

[52] S.B. Larson, J.S. Day, A. McPherson, X-ray crystallographic analyses of pig pancreatic α-amylase with limit dextrin, oligosaccharide, and α-cyclodextrin, Biochemistry 49(14) (2010) 3101-3115, https://doi.org/10.1021/bi902183w.

[53] M. Kagawa, Z. Fujimoto, M. Momma, K. Takase, H. Mizuno, Crystal structure of *Bacillus subtilis* α-amylase in complex with acarbose, J. Bacteriol. 185(23) (2003) 6981-6984, https://doi.org/10.1128/Jb.185.23.6981-6984.2003.

[54] N. Aghajari, M. Roth, R. Haser, Crystallographic evidence of a transglycosylation reaction: ternary complexes of a psychrophilic α-amylase, Biochemistry 41(13) (2002) 4273-4280, https://doi.org/10.1021/bi0160516.

[55] J. Sevcik, E. Hostinova, A. Solovicova, J. Gasperik, Z. Dauter, K.S. Wilson, Structure of the complex of a yeast glucoamylase with acarbose reveals the presence of a raw starch binding site on the catalytic domain, FEBS J. 273(10) (2006) 2161-2171, https://doi.org/10.1111/j.1742-4658.2006.05230.x.

[56] K. Lorentz, Evaluation of α-amylase assays with 4-nitrophenyl-α-oligosaccharides as substrates, J. Clin. Chem. Clin. Biochem. 21(7) (1983) 463-471, https://doi.org/10.1515/cclm.1983.21.7.463.

[57] J. Alikhajeh, K. Khajeh, B. Ranjbar, H. Naderi-Manesh, Y.H. Lin, E. Liu, H.H. Guan, Y.C. Hsieh, P. Chuankhayan, Y.C. Huang, J. Jeyaraman, M.Y. Liu, C.J. Chen, Structure of *Bacillus amyloliquefaciens* α-amylase at high resolution: implications for thermal stability, Acta Cryst. F. 66(Pt 2) (2010) 121-129, https://doi.org/10.1107/S1744309109051938.

[58] T. Shirai, K. Igarashi, T. Ozawa, H. Hagihara, T. Kobayashi, K. Ozaki, S. Ito, Ancestral sequence evolutionary trace and crystal structure analyses of alkaline α-amylase from *Bacillus* sp. KSM-1378 to clarify the alkaline adaptation process of proteins, Proteins: Struct. Funct. Bioinf. 66(3) (2007) 600-610, https://doi.org/10.1002/Prot.21255.

[59] R. Kanai, K. Haga, T. Akiba, K. Yamane, K. Harata, Biochemical and crystallographic analyses of maltohexaose-producing amylase from alkalophilic *Bacillus* sp. 707, Biochemistry 43(44) (2004) 14047-14056, https://doi.org/10.1021/Bi048489m.

[60] D. Suvd, Z. Fujimoto, K. Takase, M. Matsumura, H. Mizuno, Crystal structure of *Bacillus stearothermaphilus* α-amylase: Possible factors determining the thermostability, J. Biochem. 129(3) (2001) 461-468, https://doi.org/10.1093/oxfordjournals.jbchem.a002878.

[61] W.A. Offen, A. Viksoe-Nielsen, T.V. Borchert, K.S. Wilson, G.J. Davies, Three-dimensional structure of a variant `Termamyl-like' *Geobacillus stearothermophilus* α-amylase at 1.9 A resolution, Acta Cryst. F. 71(Pt 1) (2015) 66-70, https://doi.org/10.1107/S2053230X14026508.

[62] T. Nonaka, M. Fujihashi, A. Kita, H. Hagihara, K. Ozaki, S. Ito, K. Miki, Crystal structure of calcium-free α-amylase from *Bacillus* sp. strain KSM-K38 (AmyK38) and its sodium ion binding sites, J. Biol. Chem. 278(27) (2003) 24818-24824, https://doi.org/10.1074/jbc.M212763200.

[63] T.C. Tan, B.N. Mijts, K. Swaminathan, B.K.C. Patel, C. Divne, Crystal structure of the polyextremophilic α-amylase AmyB from *Halothermothrix orenii*: Details of a productive enzyme-substrate complex and an N domain with a role in binding raw starch, J. Mol. Biol. 378(4) (2008) 852-870, https://doi.org/ 10.1016/j.jmb.2008.02.041.

[64] S. Bozonnet, M.T. Jensen, M.M. Nielsen, N. Aghajari, M.H. Jensen, B. Kramhoft, M. Willemoes, S. Tranier, R. Haser, B. Svensson, The 'pair of sugar tongs' site on the non-catalytic domain C of barley α-amylase participates in substrate binding and activity, FEBS J. 274(19) (2007) 5055-5067, https://doi.org/10.1111/j.1742-4658.2007.06024.x.

[65] A. Vujicic-Zagar, B.W. Dijkstra, Monoclinic crystal form of *Aspergillus niger* α-amylase in complex with maltose at 1.8 angstroms resolution, Acta Cryst. F. 62(Pt 8) (2006) 716-721, https://doi.org/10.1107/S1744309106024729.

[66] G. Arnal, D.W. Cockburn, H. Brumer, N.M. Koropatkin, Structural basis for the flexible recognition of α-glucan substrates by *Bacteroides thetaiotaomicron* SusG, Prot. Sci. 27(6) (2018) 1093-1101, https://doi.org/10.1002/pro.3410.

[67] Z. Fujimoto, K. Takase, N. Doui, M. Momma, T. Matsumoto, H. Mizuno, Crystal structure of a catalytic-site mutant α-amylase from *Bacillus subtilis* complexed with maltopentaose, J. Mol. Biol. 277(2) (1998) 393-407, https://doi.org/10.1006/jmbi.1997.1599.

Journal Pre-proof

Table 1. Data collection and refinement statistics. Numbers in parenthesis are for the highest resolution shell.

	wt *Bli*Amy	ACR-MAL	MAL	G6	β-CD
Data collection					
Unit cell a, c (Å)	83.5, 188.5	83.1, 188.1	83.0, 187.4	82.1, 186.3	82.9, 187.2
Resolution (Å)	1.95	1.93	2.04	1.94	1.93
No. of observations	361367 (24852)	486367 (18832)	343755 (17936)	385962 (17936)	377706 (17047)
No. of unique reflections	49554 (3415)	49402 (2263)	42384 (2385)	48251 (2575)	49463 (2544)
R_{pim} (%)	4.7 (31.8)	4.4 (19.9)	5.8 (25.7)	7.1 (37.8)	7.1 (33.0)
CC(1/2) (%)	99.3 (63.7)	99.7 (78.1)	99.5 (80.5)	99.4 (62.3)	99.3 (60.9)
Completeness (%)	100 (100)	97.6 (68.0)	99.2 (76.3)	98.6 (79.9)	98.5 (77.1)
Mean I/σ (I)	11.1 (2.2)	13.5 (3.5)	11.1 (2.8)	8.3 (1.8)	7.8 (2.0)
Redundancy	7.3 (7.3)	9.8 (8.3)	8.1 (7.5)	8.0 (7.0)	7.6 (6.7)
Wilson *B* factor ($Å^2$)	21.1	12.4	12.5	14.2	9.7
Refinement					
R / Rfree (%)	17.0 / 20.4	15.3 / 18.1	15.6 / 18.5	16.4 / 20.1	17.1 / 20.0
Ligand active site	malonate	acarbose	malonate	malonate	malonate
Ligand remote site	-	acarbose	maltose	maltotetraose	β-CD
Waters	475	468	405	403	419
Geometry:					
RMSD Bond lengths (Å)	1.48	1.41	1.39	1.46	1.46
RMSD Bond angles (°)	0.011	0.010	0.010	0.011	0.011
Ramachandran favored (%)	96.7	96.9	97.1	96.7	96.9
Ramachandran outliers (%)	0.0	0.0	0.0	0.0	0.0
Molprobity score	1.14	0.97	1.07	0.99	0.96
PDB accession code	6TOY	6TOZ	6TP0	6TP1	6TP2

Abbreviations used: ACR = acarbose, β-CD = β-cyclodextrin, MAL= maltose, G6=maltohexaose.

Journal Pre-proof

Table 2. Overview of GH 13 structures covered in the present paper.

GH13 subfamily	Id. (%)	Rmsd (Å)	PDB	Reference
GH13_5				
	95	0.4	1BLI	[33]
Bacillus licheniformis	95	0.8	1OB0	[41]
(AmyA, AmyL, AmyS, or BLA)	94	0.6	1BPL	[40]
	96	0.5	1VJS	[39]
Chimera (BA2)	85	0.5, 0.6 0.5, 0.4	1E40, 1E3X, 1E3Z, 1E43	[43]
Bacillus amyloliquefaciens (Amy1;AmyQ;BAA)	80	0.5	3BH4	[57]
Bacillus halmapalus (BHA)	72	0.7	2GJP, 2GJR, 1W9X	[46] [42]
Bacillus sp. KSM-1378 (AmyK)	69	0.7	2DIE	[58]
Bacillus sp. 707 (AmyG6)	69	0.7	1WP6, 1WPC 2D3N, 2D3L	[59] [44]
Bacillus stearothermophilus STB04 (Bst-MFA)	66	0.6	6AG0	[45]
Geobacillus stearothermophilus (AmyS)	65	0.8	1HVX 4UZU	[60] [61]
Alicyclobacillus sp 18711 (AliC)	64	0.6	6GYA, 6GXV	[47]
Bacillus sp. KSM-K38 (AmyK38)	63	0.7	1UD3, 1UD5, 1UD8, 1UD4, 1UD6, 1UD2	[62]
Halothermothrix orenii (AmyB)	44	1.4	3BCF, 3BC9, 3BCD	[63]
GH13_6				
Hordeum vulgare (Barley)	28	2.3	2QPU	[64]
GH13_1				
Aspergillus niger	20	2.7	2GVY, 2GUY	[65]
GH13_24				
Porcine Pancreatic			3L2M	[52]
Human Pancreatic	18		5TD4	[17]
GH13_7				
Pyrococcus woesei (PWA)	33	2.1	3QGV	(Hein et al. unpubl.)
			1MWO, 1MXD, 1MXG	[48]
GH13_32				
Alteromonas haloplanctis	17	2.4	1G94	[54]
GH13 no subfamily				
Bacteroides thetaiotaomicron (SuSG)	20	2.7	3K8K, 3K8L, 3K8M 6BS6	[16] [66]
GH13_28				
Bacillus subtilis 2633	21	2.9	1BAG, 1UA7	[67] [53]

Journal Pre-proof

Table 3. Determinant residues for SBS

GH13_5	PDB ID	Ligand	38	96	98	255	257	318	319	355	356	358
*Bli*Amy *B. paralicheniformis*		MTT MAL ACR β-CD	T	N	Y	E	F	V	K	E	A	Y
B. licheniformis (BLA)	1BLI	-	T	N	Y	E	F	L	K	E	S	Y
Chimeric (BA2)	1E40	MLR	T	Q	Y	E	F	L	K	E	S	Y
B. amyloliquefaciens	3BH4	-	T	Q	Y	E	F	E	K	E	S	Y
B. halmapalus	2GJP	GLC	T	Q	Y	E	F	M	H	E	Q	Y
Bacillus sp. KSM-1378 (AmyK)	2DIE	-	T	Q	Y	P	F	I	H	E	Q	Y
Bacillus sp. 707	2D3N, 2D3L	MLR	T	Q	Y	N	F	S	H	E	Q	Y
B.stearothermophilus STB04 (Bst-MFA)	6AG0	ACR	T	Q	Y	P	F	T	L	Q	E	Y
G. stearothermophilus (AmyS)	4UZU	-	T	Q	Y	P	F	T	L	Q	E	Y
Alicyclobacillus sp. 18711 (AliC)	6GYA, 6GXV	MAL GLC	T	Q	Y	N	F	I	Q	Q	E	Y
Bacillus sp. KSM-K38 (AmyK38)	1UD2	-	T	N	Y	D	F	M	H	E	G	Y
H. orenii (AmyB)	3BCD	-	T	K	Y	D	F	N	R	E	E	V
Other members GH13												
B. thetaiotaomicron (SUSG)	3K8K	-	K	K	Y	D	Y	-	I	D	A	H
P. woesei	1MXG	ACR	S	K	I	-	W	F	K	-	E	Q
Alteromonas haloplanctis	1G94	-	A	D	Y		L	S				Y

Abbreviations used: ACR = acarbose, β-CD = β-cyclodextrin, GLC= glucose, MAL= maltose, MLR = maltotriose, MTT = maltotetraose.

Journal Pre-proof

Table 4. Catalytic efficiencies of *Bli*Amy variants for hydrolysis of soluble starch, pNP-G6 and starch granules.

	Soluble starch			pNP-G6			Starch granules
	k_{cat} (x 10^3 s^{-1})	K_m (mg/mL)	k_{cat} /K_m (s^{-1}/ mg/mL) (%)	k_{cat} (min^{-1})	K_m (mM)	k_{cat} /K_m (min^{-1}/ mM) (%)	k_{cat} /K_m (s^{-1}/ mg/mL) (%)
Wild type	1.19 ± 0.06	15.2 ± 1.5	78.3 (100)	2.02 ± 0.25	0.52 ± 0.18	3.9 (100)	2.17 ± 0.07 (100)
F257A	1.24 ± 0.08	26.2 ± 3.1	47.3 (60)	1.31 ± 0.13	0.31 ± 0.08	4.2 (108)	1.29 ± 0.04 (59)
Y358A	1.19 ± 0.05	13.3 ± 1.2	89.5 (114)	1.46 ± 0.11	0.28 ± 0.08	5.2 (134)	1.08 ± 0.07 (50)
F257A/Y358A	0.53± 0.02	14.3 ± 1.2	37.1 (47)	0.40 ± 0.02	0.08 ± 0.02	5 (128)	0.44 ± 0.01 (20)

Journal Pre-proof

Figure captions

Fig. 1. Cartoon representation of the crystal structure of *Bacillus paralicheniformis* strain ATCC 9945a amylase (*Bli*Amy) with a zoomed-in window of the active site (on the right side). The three domains A, B and C are colored green, red and yellow, respectively. The inhibitor acarbose indicated in cyan is bound at subsites -1 to +3 of the active site with the proton donor and acceptor shown in yellow. Acarbose binding at the remote surface binding site (SBS), at the bottom of the (β/α)8-barrel A domain, is shown in violet. The remotely bound acarbose molecule at the other side of where the active site is located, with a distance of ~35 Å, is indicated by the curved black arrow. Calcium ions are depicted in green and sodium ions in purple.

Fig. 2. Views of the SBS of *Bli*Amy in complex with oligosaccharides or oligosaccharide precursors. A) acarbose, B) maltose, C) β-cyclodextrin, D) maltohexaose. F257 and Y358 are shown in cyan sticks. Hydrogen bonds are shown as dotted lines.

Fig. 3. Examples of various SBSs of GH13_5 amylases. A. AmyG6 (PDB 2D3N) W140 and W167 stack with the oligosaccharide molecules at subsites -5 and -6 of the active site [59]. B. W187 of AliC (PDB 6GXV) in complex with glucose [47]. C. A maltose molecule is stacked on W347 in BHA (PDB 2GJP). D. BHA with a glucose molecule stacking on the platform of W439 and W469. E. G6 has a maltose binding site near W284. F. Bst-MFA (PDB 6AG0) in complex with acarbose near the conserved Y159. Calcium ions are depicted in green and sodium ions in purple. *Bli*Amy probably has additional SBSs as shown in panel A – C but sugar binding is not observed in our structures since these residues are involved in crystal formation. SBSs shown in panels D – F are not conserved in *Bli*Amy

Fig. 4. Examples of various SBSs of other GH13 amylases. A. SBS1 (starch granule binding site) in barley α-amylase (PDB 2QPU) comprised of W278 and W279. B. SBS2 (pair of sugar tongs binding site) involving Y380 and H395 in barley α-amylase [14, 49]. C. Aromatic platform including W460 and Y469 of the A domain of SusG (PDB 6BS6) [16, 66]. These SBSs are not conserved in *Bli*Amy

Fig. 5. Hydrolysis of raw corn starch granules by *Bli*Amy variants. -●- WT, -■- F257A, -▲- Y358A, -▼- F257A/Y358A.

Fig. 6. Binding of *Bli*Amy variants to corn starch granules. -▼- WT, -●- F257A, -▲- Y358A, -■- F257A/Y358A.

International Journal of Biological Macromolecules, Bozic et al., Fig. 1

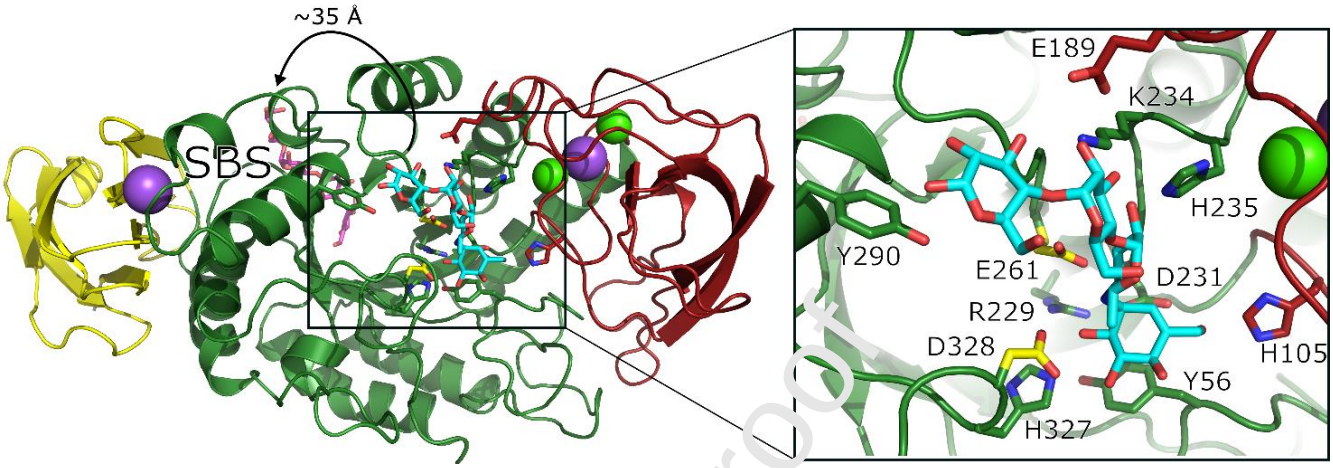

Journal Pre-proof

International Journal of Biological Macromolecules, Bozic et al., Fig. 2

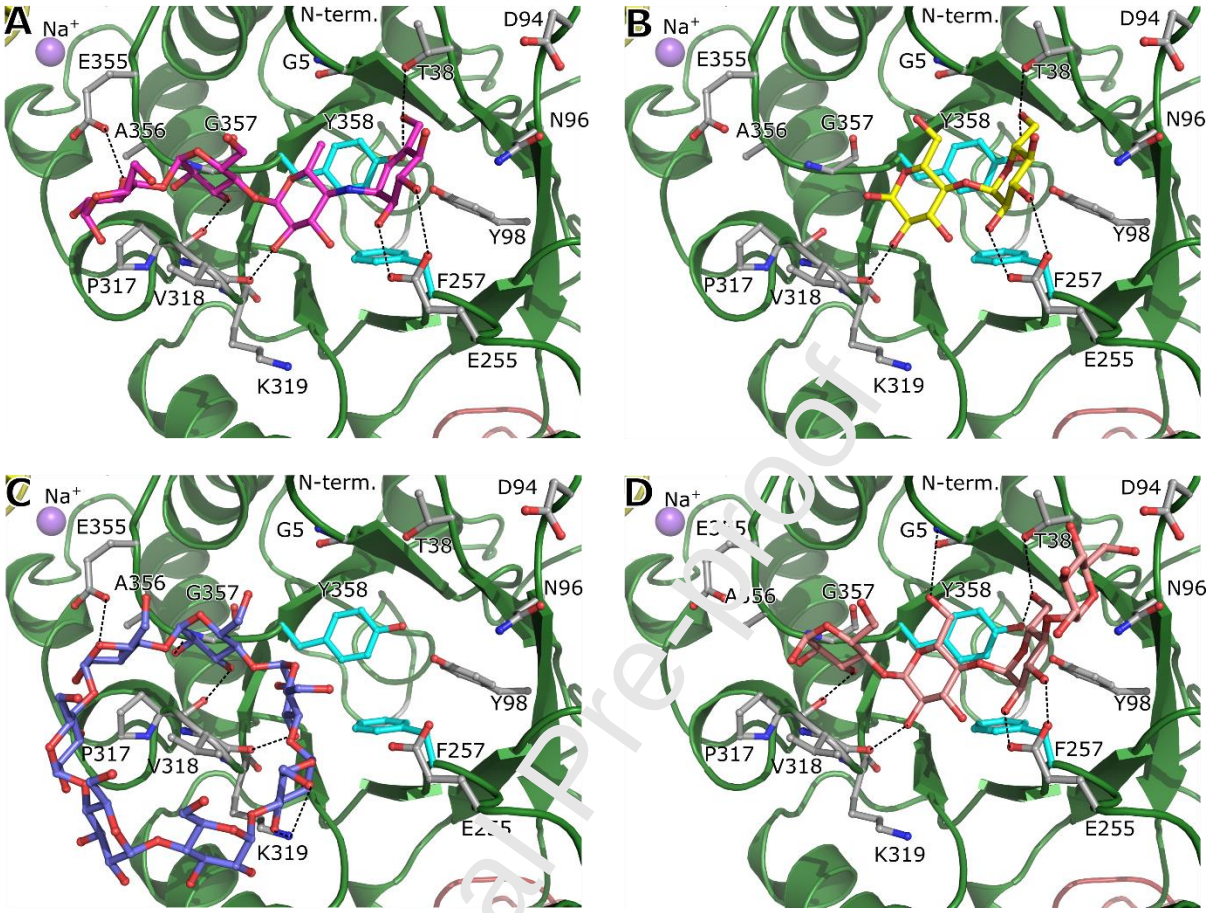

Journal Pre-proof

International Journal of Biological Macromolecules, Bozic et al., Fig. 3

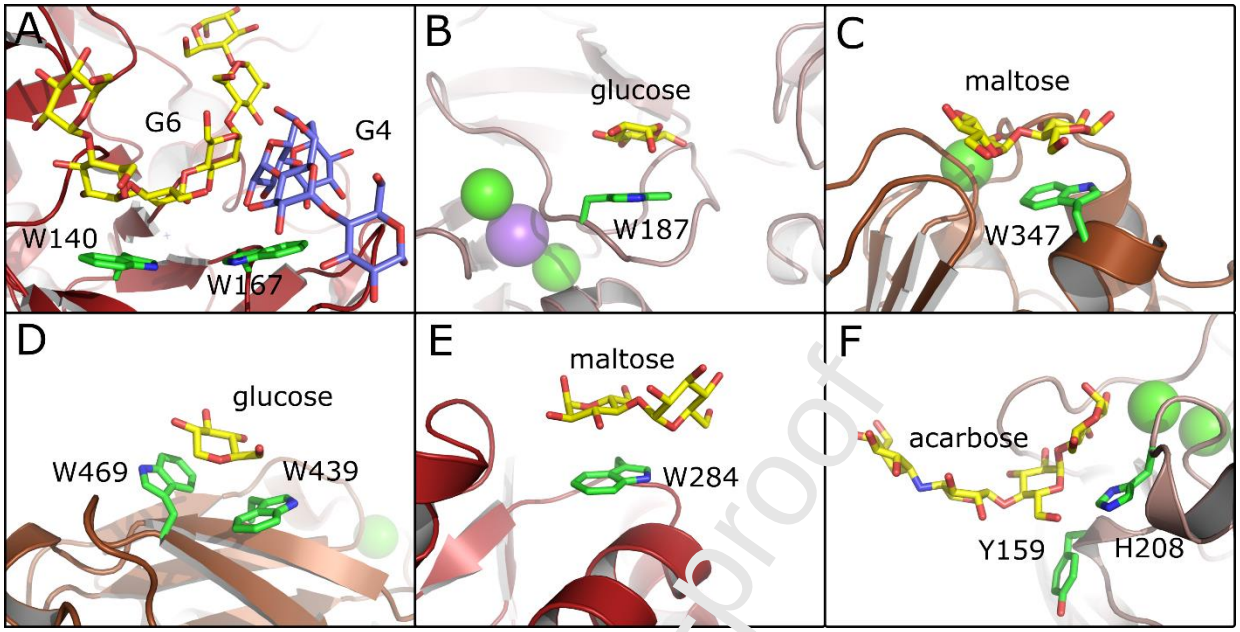

Journal Pre-proof

International Journal of Biological Macromolecules, Bozic et al., Fig. 4

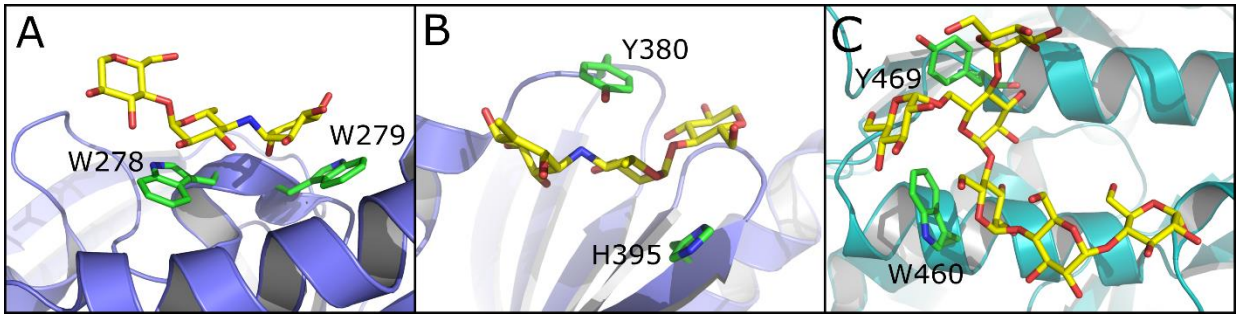

Journal Pre-proof

International Journal of Biological Macromolecules, Bozic et al., Fig. 5

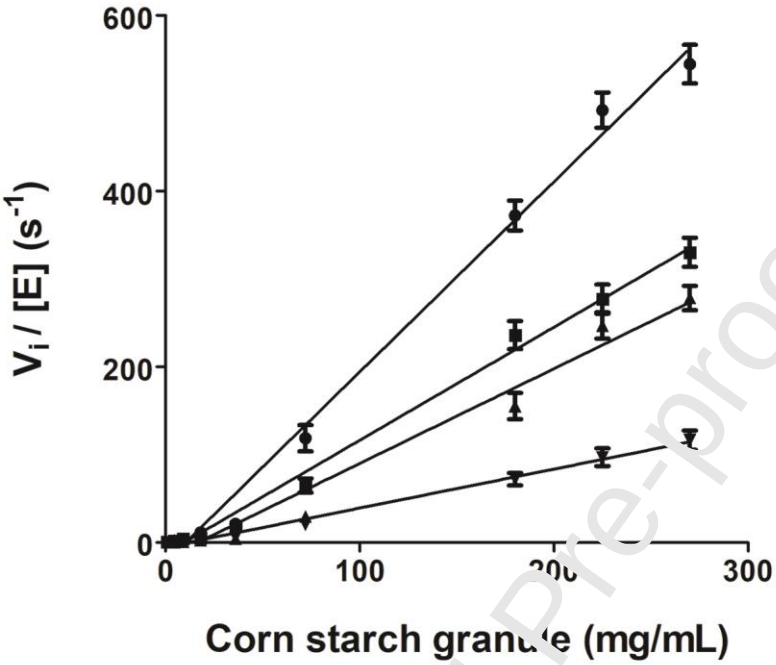

Journal Pre-proof

International Journal of Biological Macromolecules, Bozic et al., Fig. 6

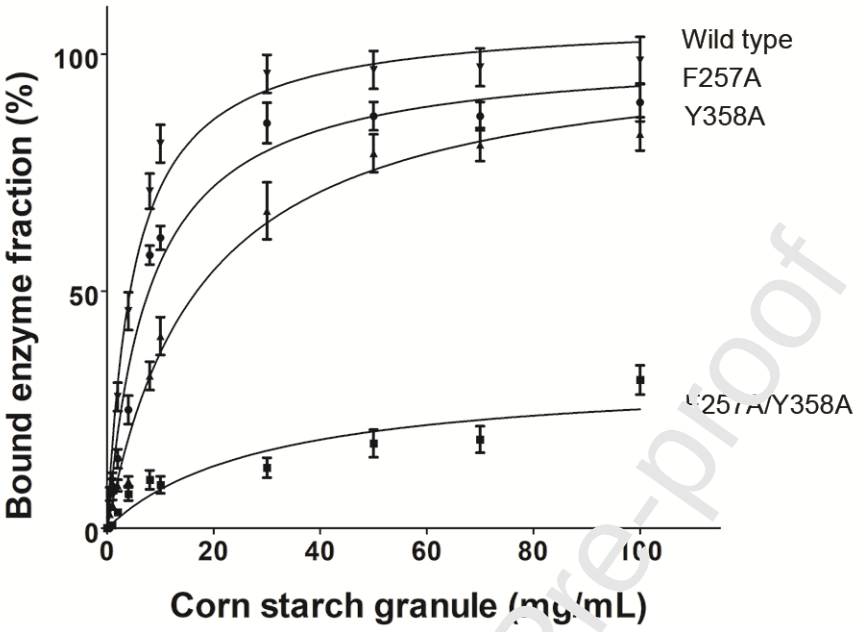

	K_d (mg/mL)
Wild type	4.96 ± 0.78
F257A	7.93 ± 1.32
Y358A	17.52 ± 2.49
F257A/Y358A	29.77 ± 6.57

Journal Pre-proof

Author statement

Submission of an article implies: that the work described has not been published previously; that it is not under consideration for publication elsewhere; that its publication is approved by all authors, and tacitly or explicitly by the responsible authorities where the work was carried out, and that, if accepted, it will not be published elsewhere in the same form, in English or in any other language, including electronically without the written consent of the copyright holder. All authors have seen and approved the final version of the manuscript being submitted. The authors declare that they have no known competing financial interests or personal relationships that could have appeared to influence the work reported in this paper.

Journal Pre-proof

Highlights

- Structure determination of *Bacillus paralicheniformis* α-amylase ATCC 9945a
- Binding of four different oligosaccharides and oligosaccharide precursors
- Confirmation of the unusual starch binding site on the α-amylase
- Verification of the starch binding site by mutational analysis

Journal Pre-proof